Izvestiya Vysshikh Uchebnykh Zavedeniy. Applied Nonlinear Dynamics. 2022;30(1)

Article
DOI: 10.18500/0869-6632-2022-30-1-7-29

Generalized Rabinovich–Fabrikant system: equations and its dynamics

S. P. Kuznetsov, *Turukina L. V.*✉

Saratov State University, Russia
Saratov Brunch of Kotelnikov Institute of Radioengineering
and Electronics of RAS, Russia
E-mail: ✉turukinalv@yandex.ru
Received 25.06.2021, accepted 10.08.2021, published 31.01.2022

Abstract. *The purpose* of this work is to numerically study of the generalized Rabinovich–Fabrikant model. This model is obtained using the Lagrange formalism and describing the three-mode interaction in the presence of a general cubic nonlinearity. The model demonstrates very rich dynamics due to the presence of third-order nonlinearity in the equations. *Methods.* The study is based on the numerical solution of the obtained analytically differential equations, and their numerical bifurcation analysis using the MatCont program. *Results.* For the generalized model we present a charts of dynamic regimes in the control parameter plane, Lyapunov exponents depending on parameters, portraits of attractors and their basins. On the plane of control parameters, bifurcation lines and points are numerically found. They are plotted for equilibrium point and period one limit cycle. It is shown that the dynamics of the generalized model depends on the signature of the characteristic expressions presented in the equations. A comparison with the dynamics of the Rabinovich–Fabrikant model is carried out. We indicated a region in the parameter plane in which there is a complete or partial coincidence of dynamics. *Conclusion.* The generalized model is new and describes the interaction of three modes, in the case when the cubic nonlinearity that determines their interaction is given in a general form. In addition, since the considered model is a certain natural extension of the well-known Rabinovich–Fabrikant model, then it is universal. And it can simulate systems of various physical nature (including radio engineering), in which there is a three-mode interaction and there is a general cubic nonlinearity.

Keywords: Rabinovich–Fabrikant model, chaotic attractors, Lagrange formalism, bifurcation analysis, multistability.

Acknowledgements. Research was carried out under support of the Russian Science Foundation (project no. 21-12-00121), https://rscf.ru/project/21-12-00121/

For citation: Kuznetsov SP, Turukina LV. Generalized Rabinovich–Fabrikant system: equations and its dynamics. Izvestiya VUZ. Applied Nonlinear Dynamics. 2022;30(1):7–29. DOI: 10.18500/0869-6632-2022-30-1-7-29

Introduction

One of the fundamental interdisciplinary problems is the study of the complex dynamics of nonlinear systems, including dynamic chaos. To date, extensive material has been accumulated, including many theoretical results, methods and algorithms of analysis, a variety of examples of model systems with complex dynamics, experimental data, etc. [1–10]. A productive approach in this direction consists in the development of generalized models that cover a particular range of phenomena and are applicable, at least for the qualitative description of systems of various

nature. One of these models was proposed in 1979 . Rabinovich and the Fabricant [11] for the description of modulation instability and the occurrence of chaos in the parametric interaction of modes in a nonequilibrium dissipative medium with cubic nonlinearity with spectrally narrow gain. It is believed that three modes are excited — the main mode falling into the instability region, and two symmetrically located satellites outside this region. The problem is reduced under a number of simplifying assumptions to a finite-dimensional system of differential equations with respect to three real variables

$$\begin{aligned} \dot{x} &= y(z - 1 + x^2) + \gamma x, \\ \dot{y} &= x(3z + 1 - x^2) + \gamma y, \\ \dot{z} &= -2z(\nu + xy), \end{aligned} \tag{1}$$

where x, y, z are dynamic variables, and ν and γ – parameters.

It is known that the Rabinovich–Fabricant model demonstrates a rich phenomenology of dynamic behavior. It includes various regular and chaotic modes and multistability, when attractors of different types coexist in the phase space [12–20]. The model has a universal character in the sense that it covers many systems of different physical nature, such as, for example, Tollmin waves– of Schlichting in hydrodynamic currents [21], wind waves on water [22], waves in chemical media with diffusion [23], and also parametric oscillations realized in a radio engineering device [18].

In this paper, we propose some natural extension of the Rabinovich–Fabricant model, in which the cubic nonlinearity defining the interaction of the three modes is given in a more general form. It can be assumed that the use of a generalized model will expand the scope of the approach proposed in the work of Rabinovich–Fabricant, and the phenomenology of the observed dynamic behavior.

1. Derivation of the generalized model equations

Note that the Rabinovich–Fabricant model can be interpreted as the result of applying the method of slow amplitudes to a system of three oscillators described by the Lagrange function

$$L(x, y, z) = \frac{1}{2} \sum_{n=0}^{2} \left(m_n \dot{x}_n^2 - k_n x_n^2 \right) - U\left(x_0, x_1, x_2\right), \tag{2}$$

where the interaction potential $U(x_0, x_1, x_2)$ is given by a fourth-degree polynomial in its three arguments and dissipation is added, determined by the Rayleigh function with coefficients positive for satellites and negative for the main mode:

$$R = \frac{1}{2} \left(-\gamma_0 \dot{x}_0^2 + \gamma_1 \dot{x}_1^2 + \gamma_2 \dot{x}_2^2 \right). \tag{3}$$

With respect to the nonlinear interaction, we will assume that it is completely symmetric with respect to the permutation of oscillators, that is, the function $U(x_0, x_1, x_2)$ is represented as the sum of all possible combinations of the fourth degree of generalized coordinates. Due to the symmetry, the potential function is naturally constructed as the sum of four groups of similar

terms, each of which can have its own constant coefficient.:

$$U(x_0,x_1,x_2)=\Big[\frac{1}{4}\left(x_0^4+x_1^4+x_2^4\right)+3\beta\left(x_0^2x_1^2+x_0^2x_2^2+x_1^2x_2^2\right)+ \\ +3\mu\left(x_0^2x_1x_2+x_1^2x_0x_2+x_2^2x_0x_1\right)+ \\ +\eta\left(x_0^3x_1+x_0^3x_2+x_1^3x_0+x_1^3x_2+x_2^3x_0+x_2^3x_1\right)\Big]. \tag{4}$$

The constants μ, β, η act as dimensionless parameters characterizing nonlinearity. As we will see later, the parameter η turns out to be insignificant when moving to the description within the framework of the slow amplitude method. The traditional model Rabinovich – Fabricant is obtained under the assumption $\mu=\beta=1$.

Lagrange equations

$$\frac{d}{dt}\left(\frac{\partial L}{\partial\dot{x}_j}\right)-\frac{\partial L}{\partial x_j}=-\frac{\partial L}{\partial\dot{x}_j},\quad j=0,1,2 \tag{5}$$

explicitly written as

$$\begin{aligned}
&m_0\ddot{x}_0+k_0x_0+\alpha\left[x_0^3+3\beta x_0\left(x_1^2+x_2^2\right)+3\mu x_1x_2\left(2x_0+x_1+x_2\right)+\right. \\
&\qquad\left.+\eta\left(3x_0^2x_1+3x_0^2x_2+x_1^3+x_2^3\right)\right]=\gamma_0\dot{x}_0, \\
&m_1\ddot{x}_1+k_1x_1+\alpha\left[x_1^3+3\beta x_1\left(x_2^2+x_0^2\right)+3\mu x_2x_0\left(2x_1+x_2+x_0\right)+\right. \\
&\qquad\left.+\eta\left(3x_1^2x_0+3x_1^2x_2+x_0^3+x_2^3\right)\right]=-\gamma_1\dot{x}_1, \\
&m_2\ddot{x}_2+k_2x_2+\alpha\left[x_2^3+3\beta x_2\left(x_0^2+x_1^2\right)+3\mu x_0x_1\left(2x_2+x_0+x_1\right)+\right. \\
&\qquad\left.+\eta\left(3x_2^2x_0+3x_2^2x_1+x_0^3+x_1^3\right)\right]=-\gamma_2\dot{x}_2.
\end{aligned} \tag{6}$$

Here the oscillator with the index 0 corresponds to the main mode, and the satellites — respectively, 1 and 2.

Bearing in mind the imposed resonant condition $2\omega_0\approx\omega_1+\omega_2$, where $\omega_i=\sqrt{k_i/m_i}$, under the assumption of low nonlinearity and dissipation, we can assume that the amplitudes of the modes change insignificantly over a characteristic time interval, and apply the method of slow amplitudes to the system (6). To do this , we present the generalized coordinates of the oscillators in the form

$$x_n=a_n\exp(i\omega_nt)+a_n^*\exp(-i\omega_nt),\qquad n=0,1,2, \tag{7}$$

where a_n — complex amplitudes. Since the total number of quantities (real and imaginary parts of a_n) becomes redundant in this case, we have the right to impose an additional condition on each complex amplitude of a_n

$$\dot{a}_n\exp(i\omega_nt)+\dot{a}_n^*\exp(-i\omega_nt)=0,\quad n=0,1,2. \tag{8}$$

After substituting expressions (7), (8) into equations (6), averaging over time and bringing similar terms, taking into account the possible frequency deviation from resonance $\Delta\omega=2\omega_0-\omega_1-\omega_2\neq0$

in the exponent, we obtain the following amplitude equations:

$$\begin{aligned}
\dot{a}_0 &= \frac{1}{2}\gamma_0 a_0 + i\frac{1}{\omega_0 m_0}\left[\mu a_0^* a_1 a_2 \exp\left(-i\Delta\omega t\right) + \frac{3}{2}\left(|a_0|^2 + 2\beta|a_1|^2 + 2\beta|a_2|^2\right) a_0\right],\\
\dot{a}_1 &= -\frac{1}{2}\gamma_1 a_1 + i\frac{1}{\omega_1 m_1}\left[\mu a_0^2 a_2^* \exp\left(i\Delta\omega t\right) + \frac{3}{2}\left(|a_1|^2 + 2\beta|a_0|^2 + 2\beta|a_2|^2\right) a_1\right],\\
\dot{a}_2 &= -\frac{1}{2}\gamma_2 a_2 + i\frac{1}{\omega_2 m_2}\left[\mu a_0^2 a_1^* \exp\left(i\Delta\omega t\right) + \frac{3}{2}\left(|a_2|^2 + 2\beta|a_0|^2 + 2\beta|a_1|^2\right) a_2\right].
\end{aligned} \tag{9}$$

Further, following the approach of [11], we believe that the amplitude of the main component a_0 is significantly greater than the amplitudes of the satellites $a_{1,2}$ and that the complex amplitudes of the satellites are the same, since due to the proximity of frequencies, the coefficients in the amplitude equations for the satellites 1 and 2 are almost the same.

We introduce the real amplitudes $A_{0,1}$ and phases $\varphi_{0,1}$ using the relations $a_0 = A_0\exp(i\varphi_0)$ and $a_1 = a_2 = A_1\exp(i\varphi_1)$, substitute these relations into the equations (9) and, separating the real and imaginary parts, we get

$$\begin{aligned}
\dot{B}_0 &= \mu B_0 B_1 \sin\varphi + 2\frac{\gamma_0}{\Delta\omega}B_0,\\
\dot{B}_1 &= -\mu B_0 B_1 \sin\varphi - \frac{\gamma_1}{\Delta\omega}B_1,\\
\dot{\varphi} &= 1 + (2\beta - 1)(B_1 - B_0) + \mu(2B_1 - B_0)\cos\varphi.
\end{aligned} \tag{10}$$

Here $B_n = 3/(m_n\omega_n\Delta\omega)\,A_n^2$, $n = 0, 1$ — normalized real amplitudes, $\varphi = 2(\varphi_0 - \varphi_1) + \Delta\omega t$ — current phase disorder, $\tau = \Delta\omega t$ — dimensionless time.

Finally, let's introduce new variables $x = \sqrt{2B_0}\cos(\varphi/2)$, $y = \sqrt{2B_0}\sin(\varphi/2)$, $z = B_1$ and time $t = \tau/2$. Let's also put $p = ((1/2)\mu + \beta - 1/2)$, $q = ((1/2)\mu - \beta + 1/2)$, $\gamma = \gamma_0/(\Delta\omega)$, $\nu = \gamma_1/(\Delta\omega)$. Then from the system (10) we get:

$$\begin{aligned}
\dot{x} &= \left[p(x^2 + z) + q(-y^2 + 3z) - 1\right] y + \gamma x,\\
\dot{y} &= \left[p(-x^2 + 3z) + q(y^2 + z) + 1\right] x + \gamma y,\\
\dot{z} &= -2z(\nu + (p + q)xy).
\end{aligned} \tag{11}$$

The system (11) will coincide with the Rabinovich model–Fabricant (1) if $p = 1$, $q = 0$ are put in the equations, and thus represents a generalization to the case of cubic nonlinearity a more general view than in the original model [11]. Note that, like the model Rabinovich – Fabricant, the system (11) has the property of symmetry with respect to the replacement of the variables $x \to -x$ and $y \to -y$.

There are two groups of parameters in the system (11). The first one is represented by the parameters γ и ν, which are identical to the parameters of the model Rabinovich – Fabricant and have the meaning of dissipation coefficients — positive for satellites and negative for the main mode. The second group is represented by the parameters p and q. These are new parameters that characterize the nonlinear interaction between oscillators in the system.

2. Dynamics of the generalized model on the plane of parameters of nonlinear interaction

Consider the dynamics of the system (11). To begin with, we will construct for it a map of dynamic modes on the plane of parameters of nonlinear interaction (p, q) for the values of

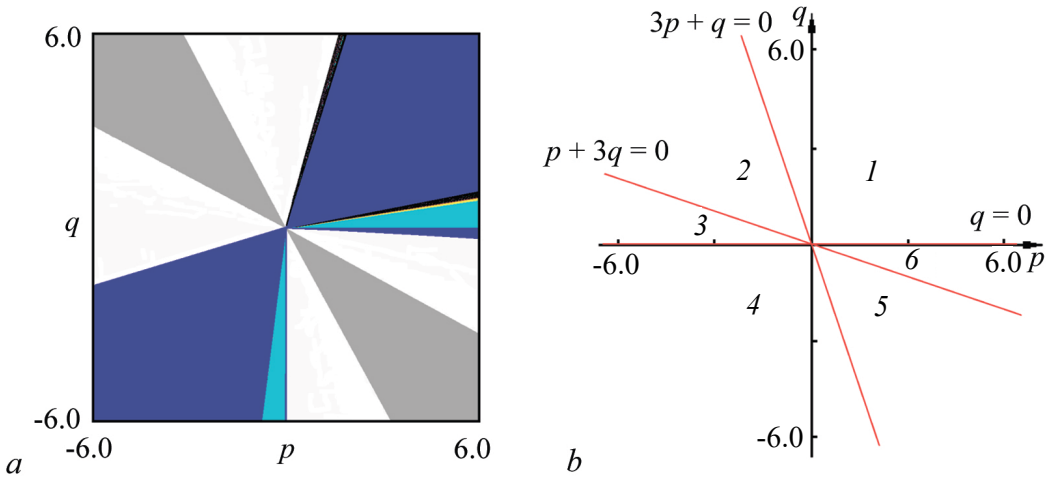

Fig. 1. *a* — Chart of dynamical regimes of the model (11) at (p, q) parameter plane at $\gamma = 0.96$ and $\nu = 1.5$. *b* — Division of the (p, q) parameter plane into regions corresponding to different signature of expressions $p + 3q$, $3p + q$ and q (color online)

parameters $\gamma = 0.96$ and $\nu = 1.5$ (Fig. 1, *a*). Such a map is constructed when scanning the parameter plane, when the type of observed mode is numerically determined at each of its points, which is indicated by the corresponding color. On the map, in Fig. 1, *a*, the following modes are observed: dark blue color corresponds to the equilibrium state, blue — to the limit cycle of the period 1, yellow — to the cycle of the period 2, red — to the cycle of the period 4, and so, the black color corresponds to the chaotic mode, and the white color indicates the area of escape of trajectories to infinity. The specified cycle periods are determined in a standard way using Poincare sections. Also, the system (11) demonstrates a new type of dynamics not observed in the model Rabinovich – Fabricant (1). It consists in the fact that in the phase space there exists an invariant (stable) set in the form of a circle lying entirely in the plane $z = 0$. The corresponding area is marked in gray on the dynamic mode map. However, this mode is not of interest for research, since in terms of the original system of differential equations (6), as follows from those variable substitutions that were made during the system output (11) (see section 1), it corresponds to the fact that the oscillator oscillation amplitude with index 0 (main mode) $A_0 = \text{const}$, and the amplitudes of oscillators with indices $1, 2$ (satellites) $A_1 = A_2 = 0$.

From Fig. 1, *a* it can be seen that the regions of various periodic regimes, chaos and the region of escape of trajectories to infinity have the form of rays diverging from the origin. At the same time, the qualitative device of the dynamic mode map of the system (11) does not depend on the choice of parameters γ and ν.

Fig. 1, *a* shows the partitioning of the plane (p, q) into regions corresponding to different signatures of expressions $p + 3q$, $3p + q$ and q. In order to explain where these expressions came from, we will rewrite the system (11) in the following form:

$$\begin{aligned} \dot{x} &= y\left[(p+3q)z - 1 + (p+q)x^2 - q\frac{x^2+y^2}{2}\right] + \gamma x, \\ \dot{y} &= x\left[(3p+q)z + 1 - (p+q)x^2 + q\frac{x^2+y^2}{2}\right] + \gamma y, \\ \dot{z} &= -2z(\nu + (p+q)xy). \end{aligned} \tag{12}$$

In this case, the equations look more cumbersome, but their structure is similar to the structure of

the equations of the Rabinovich model–Fabricant (1). Namely, in the first and second equations of the system (12) in square brackets there will be four terms of the form: $\mathrm{const}_1 z$, 1, $\mathrm{const}_2 x^2$ and a new term that was not in the model (1), $\mathrm{const}_3(x^2+y^2)$. At the same time, there are only three significant combinations of parameters in the system (12), $(p+3q)$, $(3p+q)$ and q, that is, the coefficients before the z terms in the first and second equations of the system (12) and the coefficient before the term (x^2+y^2), the same for both equations[1]. The specified conditions are set on the plane (p, q) lines:

$$p+3q=0, \quad 3p+q=0, \quad q=0, \tag{13}$$

each of which divides the plane (p, q) into two regions, in one the corresponding combination of parameters will be greater than zero, and in the other — less. The complete division of the plane (p, q) into regions is shown in Fig. 1, *b* and it, like the dynamic mode map, does not depend on the parameters γ and ν. The figure shows that the plane (p, q) is divided into six regions with different signatures of expressions $p+3q$, $3p+q$ and q. At the same time, the state of equilibrium, limit cycles of various periods and chaos will be observed only in the regions *1* ($p+3q>0$, $3p+q>0$, $q>0$), *4* ($p+3q<0$, $3p+q<0$, $q<0$) and *6* ($p+3q>0$, $3p+q>0$, $q<0$). It is from these areas that the values of the parameters p and q will be selected for further investigation of the system (11). A new type of dynamics, an invariant (stable) set in the form of a circle, lying entirely in the plane $z=0$, is located in the regions *2* ($p+3q>0$, $3p+q<0$, $q>0$) and *5* ($p+3q<0$, $3p+q>0$, $q<0$), and the escape of trajectories to infinity — in all six regions.

3. Dynamics of the generalized model on the plane of dissipation parameters

Now let's build dynamic mode maps for the system (11) on the parameter plane (ν, γ). The parameters p and q will be selected from those regions on the plane (p, q) (Fig. 1, *b*) in which the system (11) demonstrates periodic and chaotic modes, that is, from the regions *1*, *4* and *6*, as well as on the line $p=0$. The corresponding maps are shown in Fig. 2. When constructing them, the same color palette was used as in the case of Fig. 1, *a*. In addition, Fig. 2, *a* shows a map of dynamic modes for the Rabinovich – Fabricant model (1), taken from the work [20]. This will allow us to compare the dynamics of the system (11) with the dynamics characteristic of the Rabinovich – Fabricant model.

Let's first say $p=0.8$ and $q=0.0$. This corresponds to the fact that a point on the plane (p, q) lies on the line $q=0$ in Fig. 1, *b*. In this case, in the system (12), the coefficient before the summand is (x^2+y^2) is zero and from the Rabinovich – Fabricant model (1) it will differ only by other coefficients before the terms z and x^2, and the structure of the equations will be the same. The corresponding map of the dynamic modes of the system (11) on the plane (ν, γ) is shown in Fig. 2, *b*. From its comparison with Fig. 2, *a* it can be seen that the maps are both qualitatively and quantitatively identical to each other. And means that the dynamics of the system (11) will be identical to the dynamics of the system (1). Also note that for other values of the parameters p and q lying on the line $q=0$ in the region $p>0$, the map of dynamic modes of the system (11) will not change. In the case when $p<0$, in the system (11) there will be an escape of trajectories to infinity.

Now let $p=0.9$ and $q=0.1$. In this case, a point on the plane (p, q) falls into the area *1* (see Fig. 1, *b*). The corresponding map of the dynamic modes of the system (11) on the plane

[1]The fourth combination of parameters $p+q$ sets the line $p=-q$ on the plane (p, q), which is the symmetry line of the dynamic mode map, but does not affect its structure.

(ν, γ) is shown in Fig. 2, *c*, from which it can be seen that now the dynamics of the system (11) is quantitatively different from that demonstrated by the Rabinovich– Fabricant model (1) (see Fig. 2, *a*). Thus, the regions of periodic and chaotic regimes become wider and shift to the right. As we will show later, multistability will be observed at higher values of the parameter γ than in the case of the Rabinovich model–Fabricant (1).

Now let's put $p = 1.3$, and $q = -0.1$, and a point on the plane (p, q) falls into the area *6* (see Fig. 1, *b*). The map of the dynamic modes of the system (11) on the plane (ν, γ) for this case is shown in Fig. 2, *d*. It can be seen that in this case the map of dynamic modes of the system (11) differs significantly from the map constructed for the Rabinovich – Fabricant model (1) (Fig. 2, *a*): the regions of periodic and chaotic regimes have become smaller, and the area of escape of trajectories to infinity — is larger. The second structure also disappeared, demonstrating the transition to chaos through a sequence of period doubling bifurcations, which was observed at small values of the parameter γ, to the left of the main structure, and the area of multistability became narrower.

And finally, let $p = -0.05$ and $q = -0.85$. This corresponds to the fact that a point on the plane (p, q) falls into the area *4* (see Fig. 1, *b*). The corresponding map of the dynamic modes of the system (11) on the plane (ν, γ) is shown in Fig. 2, *e*. The figure shows that in this case the map of the dynamic modes of the system (11) is qualitatively identical to the map for the Rabinovich – Fabricant model (1) (see Fig. 2, *a*), although there are minor quantitative differences.

In all other regions of the plane (p, q) in the system (11), there will be either an escape of trajectories to infinity, or a new type of mode — an invariant (stable) set in the form of a circle lying entirely in the plane $z = 0$.

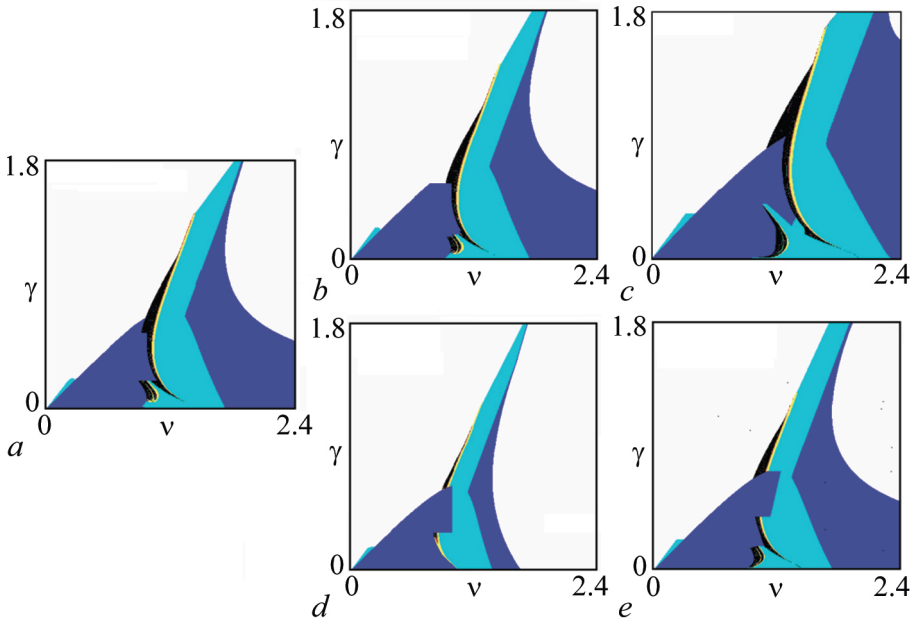

Fig. 2. *a* — Chart of dynamical regimes of the Rabinovich–Fabrikant model (1) at (ν, γ) parameter plane. *b–e* — Chart of dynamical regimes of the model (11) at (ν, γ) parameter plane at $p = 0.8$, $q = 0.0$ (*b*); $p = 0.9$, $q = 0.1$ (*c*); $p = 1.3$, $q = -0.1$ (*d*); $p = -0.05$, $q = -0.85$ (*e*) (color online)

4. The dynamics of the generalized model in the case of $p = 0.9$, $q = 0.1$

Now let's take a closer look at the dynamics of the system (11) in the case when the nonlinearity parameters take the values $p = 0.9$ and $q = 0.1$. This case is interesting because, on the one hand, the map of the dynamic modes of the system (11) (see Fig. 2, *c*) is similar to the map for the Rabinovich – Fabricant model (see Fig. 2, *a*), and on the other hand, there are a number of differences on it. As in [20], we construct for the system (11) graphs of the dependence of the spectrum of Lyapunov exponents on the parameter ν, attractors and pools of their attraction for several fixed values of the parameter γ. A we will also numerically construct bifurcation lines on the plane (ν, γ).

4.1. Case $\gamma = 0.96$. In order to make it convenient to compare the dynamics of the system (11) with the dynamics of the Rabinovich – Fabricant model (1), we choose the same values of the parameter γ. So let $\gamma = 0.96$. Fig. 3, *a* shows a graph of the dependence of three Lyapunov exponents on the parameter ν for the system (11). The figure shows that in the region of $\nu > 1.75$ all Lyapunov exponents are negative, that is, there is a stable equilibrium position in the system. The corresponding phase portrait is shown in Fig. 3, *b*. Two coexisting equilibrium positions SP are observed on it_1^- and SP_1^+, arranged symmetrically and passing into each other when x is replaced by $-x$ and y by $-y$, that is there is bistability in the (11) system. When the parameter ν decreases, stable equilibrium positions SP_1^- and SP_1^+ they disappear. In their place there are stable limit cycles CL_1^- and CL_1^+ (fig. 3, *c*), and the senior Lyapunov exponent becomes zero (see Fig. 3, *a*). With a further decrease in the parameter ν, the period of limit cycles doubles (Fig. 3, *d*, *e*), until chaotic attractors Ch arise as a result of a cascade of bifurcations of doubling the period_1^- and Ch_1^+ (Fig. 3, *f*), while the senior Lyapunov exponent will become positive.

To analyze the bistability, pools of attraction of attractors were constructed. Figure 4 shows the pools of attraction for stable equilibrium positions SP_1^- and SP_1^+, indicated in the figure in blue and green, respectively. Note that in this figure (and in all subsequent similar figures), the projection of attractors onto the plane (x, y) and the sections of the attraction basins with the plane $z_0 = \text{const}$ are presented, and the attraction basins themselves are painted in the same color as his attractor. For small values $z_0 = 0.1$, the pools of attraction of stable equilibrium positions SP_1^- and SP_1^+ they are oval areas symmetrically located relative to the origin. With the growth of z_0, the pools increase in size, and «islands» appear inside them, corresponding to the scattering of trajectories to infinity. Further, these «islands» increase in size, and the bands bounding them on the right and left become narrower and narrower, until they completely break, and peculiar «tails» appear at the pools. If we continue to increase z_0, then new «islands» appear, corresponding to the scattering of trajectories to infinity, and new «tails»; smaller areas are also separated from the main basin. In addition, with the growth of z_0 inside the basins of attraction of equilibrium positions SP_1^- and SP_1^+ narrow stripes appear, representing the pools of attraction of a symmetrical attractor (blue stripes appear inside the green area, and inside the blue — green.). For all other attractors (limit cycles of various periods, chaotic attractors) observed in this case, the pools of attraction will be qualitatively the same as for equilibrium positions SP_1^- and SP_1^+. With the only difference is that their transformations will occur at lower values of z_0, and the pools themselves will become slightly smaller.

Thus, it can be argued that with these values of the parameter γ, the dynamics of the system (11) is generally identical, at least qualitatively, to the dynamics of the model Rabinovich – Fabricant (1) [20]. There are only quantitative differences, which consist in the fact that the pools of attraction of the attractors become larger, and the same transformations in the system (11) in comparison with the model Rabinovich – Fabricant (1) occur for large values z_0. Although there

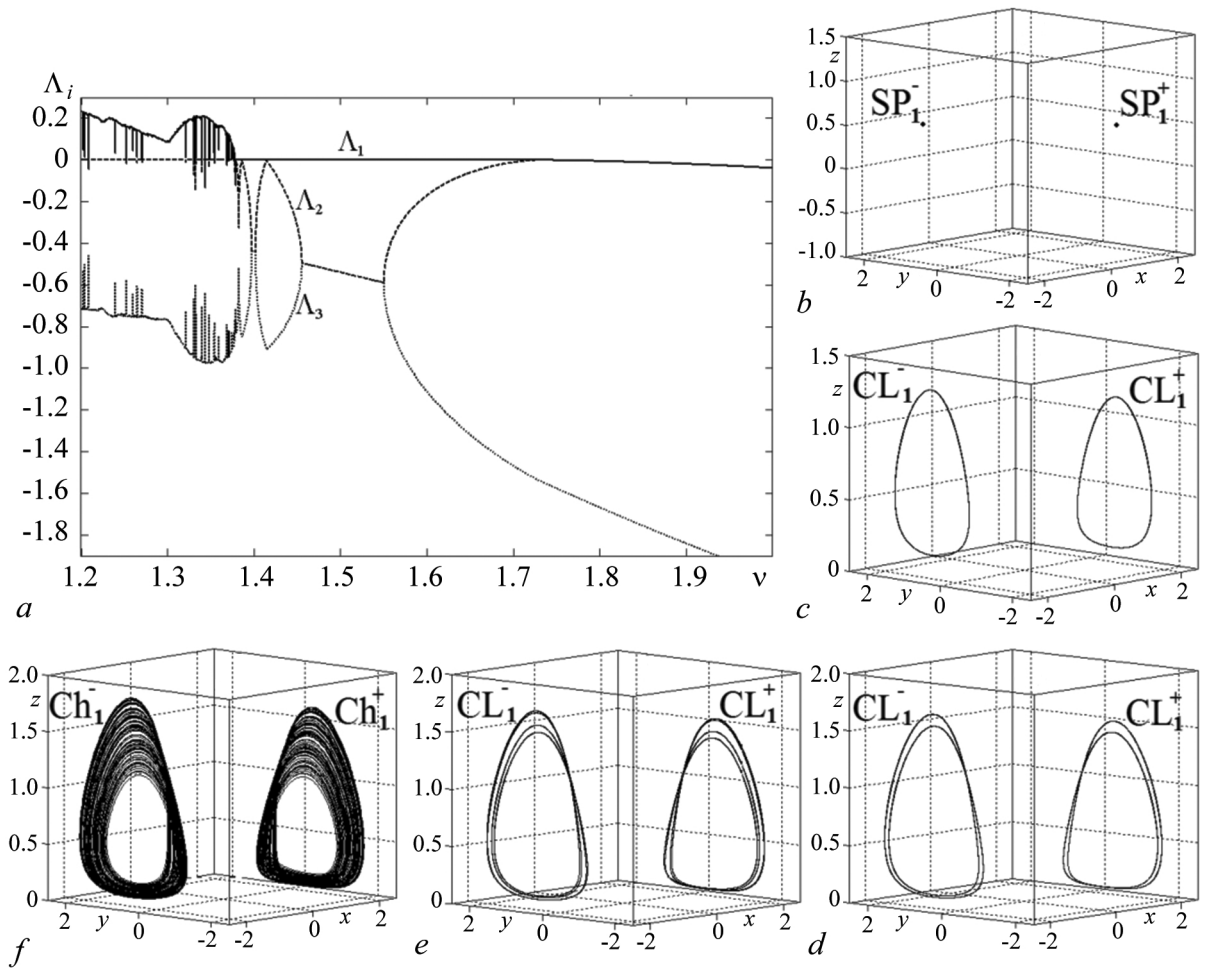

Fig. 3. *a* — Graphs of Lyapunov exponents of the model (11) on the parameter ν at $\gamma = 0.96$. *b*–*f* — Attractors of the model (11) at $\gamma = 0.96$: $\nu = 1.9$ (*b*); 1.6 (*c*); 1.4 (*d*); 1.38 (*e*); 1.35 (*f*)

is one qualitative difference, which consists in the fact that in the system (11) with the growth of z_0, narrow bands appear inside the pools of attraction, representing the pools of attraction of a symmetric attractor. No such changes were observed in the model Rabinovich – Fabricant (1).

4.2. Case $\gamma = 0.78$. Now reduce the value of the parameter γ. Let $\gamma = 0.78$. Note that the dynamics of the Rabinovich – Fabricant model will not change in this case [20]. But the dynamics of the system (11), as shown below, will be significantly different. Figure 5 shows a graph of the dependence of Lyapunov exponents on the parameter ν and the attractors of the system (11) constructed for this case. From Fig. 5, *a* it can be seen that in the area of $\nu > 1.75$ all Lyapunov exponents are negative, that is, there is a stable equilibrium position in the system. The corresponding phase portrait is shown in Fig. 5, *b*. On it, as in the previous case, two coexisting attractors SP are observed$_2^-$ and SP_2^+, footnoteStrictly speaking, these are the same equilibrium positions as SP_1^- and SP_1^+. For the convenience of presenting the material, the attractors (even if they are the same attractor) constructed for different values of the parameter γ will be indicated by their index. arranged symmetrically and passing into each other when replacing x with $-x$ and y with $-y$ [2]. When the parameter ν decreases, stable equilibrium positions SP_2^- and SP_2^+

[2]Note that due to the symmetry of the system (11), all attractors, unless otherwise specified, will arise as a symmetrically arranged pair of objects that pass into each other when x is replaced by $-x$ and y by $-y$. Therefore,

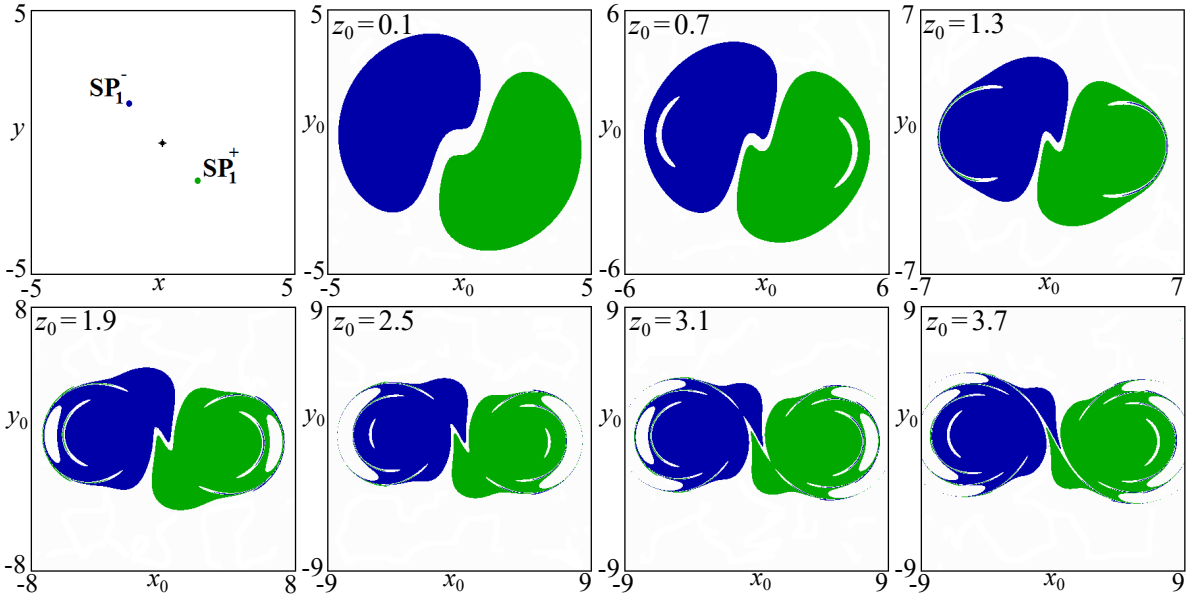

Fig. 4. Projection of the attractors on a (x, y) plane and sections of their basins by the $z_0 = \text{const}$ plane plotted for the model (11). $\gamma = 0.96$ and $\nu = 1.9$. The basin of attraction of the equilibrium position SP_1^- is colored blue, and the basin of SP_1^+ is colored green (color online)

disappear, and in their place there are stable limit cycles of CL_2^- and CL_2^+ (fig. 5, *c*), and the senior Lyapunov exponent becomes zero (see Fig. 5, *a*). With a further decrease in the parameter ν in the system (11), multistability occurs when in the phase space, in addition to stable limit cycles, CL_2^- and CL_2^+ stable equilibrium positions SP located inside them are observed.$_3^-$ and SP_3^+ (fig. 5, *d*). These new equilibrium positions do not coincide with those considered earlier and arise, as we will show later, as a result of another bifurcation. Then the period of limit cycles CL_2^- and CL_2^+ doubles (Fig. 5, *e, f*), until, as a result of a cascade of period doubling bifurcations, chaotic attractors $Charise_2^-$ and Ch_2^+ (Fig. 5, *g*), and the senior Lyapunov exponent will become positive (see Fig. 5, *a*). At the same time , stable equilibrium positions SP_3^- and SP_3^+ continue to coexist together with limit cycles and chaotic attractors until they remain the only attractors (Fig. 5, *h*) after chaotic the attractors will disappear at $\nu \approx 1.27$. Thus, in contrast to the Rabinovich – Fabricant model(1), in the system (11), with the value of the parameter $\gamma = 0.78$, multistability takes place in a certain range of variation of the parameter ν. This confirms the earlier conclusion that in the system (11) multistability is observed in a larger range of parameter changes.

Fig. 6, *a* shows the pools of attraction for stable equilibrium positions SP_2^- and SP_2^+ (see Fig. 5, *b*), indicated in the figure blue and green, respectively. From fig. 6, *a* it can be seen that for small values $z_0 = 0.1$ the pools of attraction are a circle of a rather large radius, which is divided into two parts by manifolds of an unstable equilibrium position located at the origin. In this case, the right part of the circle is the pool SP_2^+, and the left is the pool SP_2^-. With growth z_0 new regions appear both outside and inside the circle, representing the pools of attraction of the symmetric attractor (see Fig. 6, *a*). Moreover, the more z_0, the more alternating regions are observed.

Fig. 6, *b* shows pools for the case of $\nu = 1.5$, when symmetrically arranged pairs consisting of the limit cycle CL coexist in the phase space$_2^-$ (or CL_2^+) and the stable equilibrium position SP located inside it$_3^-$ (or SP_3^+) (fig. 5, *d*). In this case, at values z_0 close to zero, on the plane of the initial conditions (x_0, y_0), only pools of attraction of stable equilibrium positions SP are

this moment in the further presentation of the material will be assumed by default.

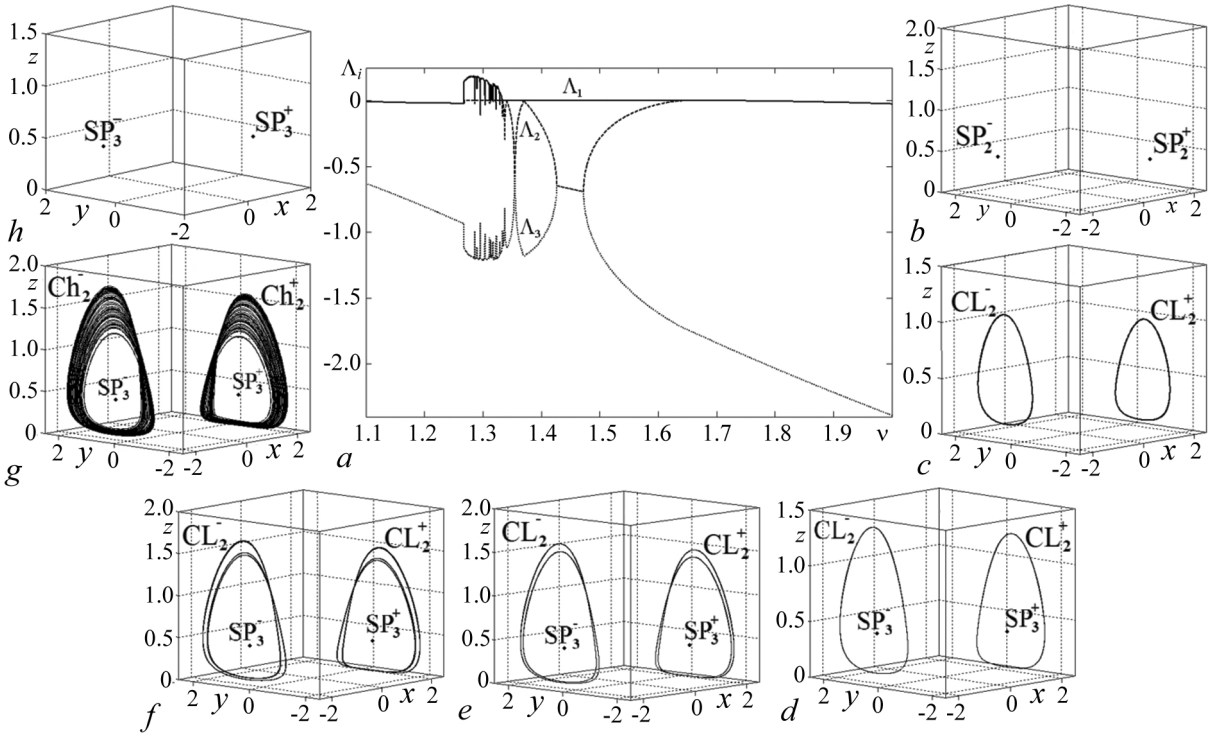

Fig. 5. *a* — Graphs of the Lyapunov exponents of the model (11) on the parameter ν at γ = 0.78. *b*–*h* — Attractors of the model (11) at γ = 0.78: ν = 2.0 (*b*); 1.6 (*c*); 1.5 (*d*); 1.36 (*e*); 1.34 (*f*); 1.3 (*g*); 1.2 (*h*)

observed$_3^-$ and SP$_3^+$, which represent oval areas symmetrically located relative to the origin. With the growth of z_0, pools of attraction of their paired limit cycles CL appear inside$_2^-$ and CL$_2^+$, which also represent oval areas. Then oval regions appear inside these regions, representing the pools of attraction of stable equilibrium positions paired with them.$_3^-$ and SP$_3^+$ and so on, etc. Thus, at $z_0 \approx 0.1$ on the plane of the initial conditions (x_0, y_0), a structure in the form of oval regions is observed (pools of attraction of stable equilibrium positions SP$_3^-$ and SP$_3^+$), inside which smaller oval regions are located (pools of attraction of the limit cycles paired with them CL$_2^-$ and CL$_2^+$), which are surrounded by narrow rings representing alternating pools of attraction of stable equilibrium positions SP$_3^-$ and SP$_3^+$ and their paired limit cycles CL$_2^-$ and CL$_2^+$. With further increase z_0 inside the attraction basins of stable equilibrium positions SP$_3^-$ and SP$_3^+$ there are «islands» corresponding to the escape of trajectories to infinity. Inside them, in turn, narrow bands appear, representing pools of attraction of a symmetrical attractor. Further, these «islands» increase in size, and the bands that limit them become narrower and narrower, until they completely break and peculiar «tails» appear at the pools. Thus, the further transformation of the pools becomes the same as in the case of γ = 0.96.

Note that the pools of attraction of the limit cycles of CL$_2^-$ and CL$_2^+$, observed at those values of the parameter ν when there is no multistability in the system (11), for example, at ν = 1.6 (see Fig. 5, *c*), are identical to the pools of attraction shown in Fig. 6, *a*. The pools of attraction for all other modes, in cases where there is multistability (see Fig. 5, *d*–*g*), will be identical to the pools of attraction shown in Fig. 6, *b*. Pools of attraction of stable equilibrium positions SP$_3^-$ and SP$_3^+$ qualitatively they will be identical to those observed in the system (11) for the case γ = 0.96 for stable equilibrium positions SP$_1^-$ and SP$_1^+$ (see Fig. 4). With the only difference that in this case the transformation of pools occurs faster, and their size grows a little slower.

Thus, the system (11) at γ=0.78 demonstrates dynamics significantly different from that in

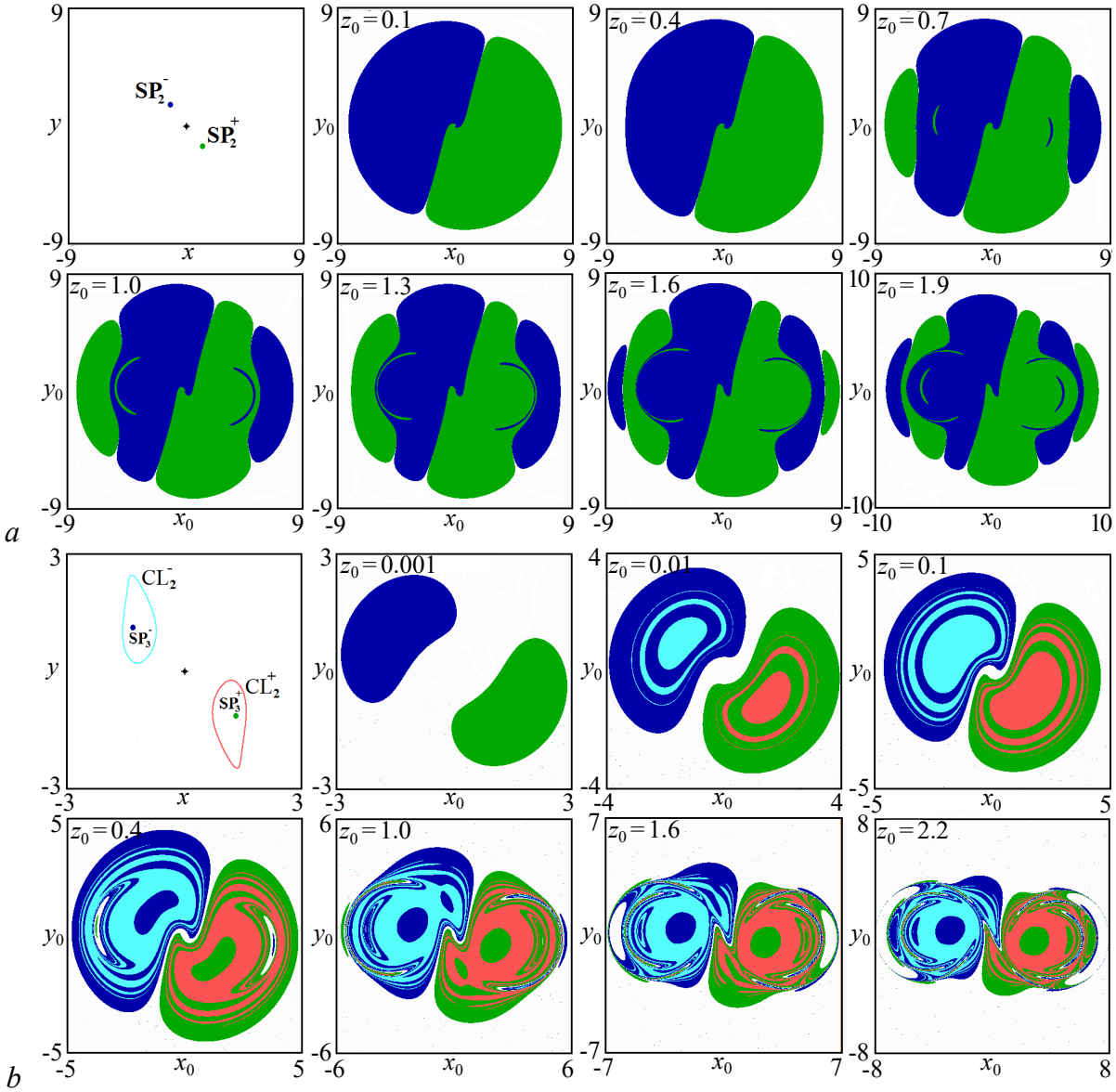

Fig. 6. Projection of the attractors on a (x, y) plane and sections of their basins of attraction by $z_0 = \text{const}$ plane plotted for the model (11). $\gamma = 0.78$, a — $\nu = 2.0$, b — $\nu = 1.5$. The basin of attraction of the equilibrium position SP_2^- is colored blue, the basin of SP_2^+ is colored green, the basin of CL_2^- is colored light blue, the basin of CL_2^+ is colored red (color online)

the Rabinovich – Fabricant model(1) at the same parameter value γ [20]. The main difference is the presence in the system (11) of multistability, which is observed in the Rabinovich – Fabricant model(1) at lower values of the parameter γ ($\gamma \approx 0.5$). At the same time, we note that if the device of the pools of attraction in the case when the system (11) has multistability, similar to what was observed in the Rabinovich – Fabricant model(1) at $\gamma = 0.5$, then the arrangement of the pools of attraction in the case when there is no multistability in the system (11) is significantly different and similar to what was observed in the Rabinovich – Fabricant model (1) at $\gamma = 0.2$.

4.3. Case $\gamma = 0.5$. Now let's say $\gamma = 0.5$. Note that the dynamics of the Rabinovich model–Fabricant (1) for a given value of the parameter γ demonstrates multistability, when two symmetrically arranged pairs co-exist in the phase space, consisting of a limit cycle and a stable equilibrium position inside it [20]. Now consider the dynamics

of the system (11). Fig. 7, *a* shows a graph of the dependence of Lyapunov exponents on the parameter ν and the attractors of the system (11) constructed for this case. The figure shows that the dynamics of the system (11) in this case is completely identical to that observed in the system (11) for $\gamma = 0.78$. Thus, at $\nu > 2.0$ and $\nu < 1.28$, stable equilibrium positions of SP are observed in the phase space$_4^-$, SP_4^+ and SP_5^-, SP_5^+ respectively (fig. 7, *b* and fig. 7, *h*); in the region $1.28 < \nu < 2.0$ — limit cycles of CL_3^- and CL_3^+, demonstrating the transition to chaos through a sequence of period doubling bifurcations (fig. 7, *c*–*g*). At the same time, with $\nu < 1.5$, multistability takes place in the system (11).

The arrangement of the pools of attraction differs significantly from what was observed for the case of $\gamma = 0.78$. Fig. 8, *a* shows the pools of attraction for stable equilibrium positions SP_4^- and SP_4^+ (see fig. 7, *b*), indicated by blue and green, respectively. From Fig. 8, *a* it can be seen that in this case the outer boundaries of the basins of attraction are complex curves. With the growth of z_0, new regions appear inside the basins, representing the basins of attraction of the symmetric attractor, first at the outer boundary, and then in the vicinity of the origin. At the same time, the size of the pools itself does not change. Note that the pools of attraction constructed for the limit cycles of CL_3^- and CL_3^+ (see Fig. 7, *c*), are completely identical to the basins for equilibrium positions SP_4^- and SP_4^+ in fig. 8, *a*. Note also that a similar arrangement of attraction pools was not observed either in the Rabinovich model – Fabricant model (1) or in the system (11) for the previously considered parameter values.

Fig. 8, *b* shows pools for the case $\nu = 1.5$, when symmetrically arranged pairs consisting of the limit cycle CL coexist in the phase space$_3^-$ (or CL_3^+) and the stable equilibrium position SP located inside it$_5^-$ (or SP_5^+) (fig. 7, *d*). From Fig. 8, *b* it can be seen that the pools of attraction of equilibrium positions SP_5^- and SP_5^+ are, as in the case of equilibrium positions SP_2^- and SP_2^+,

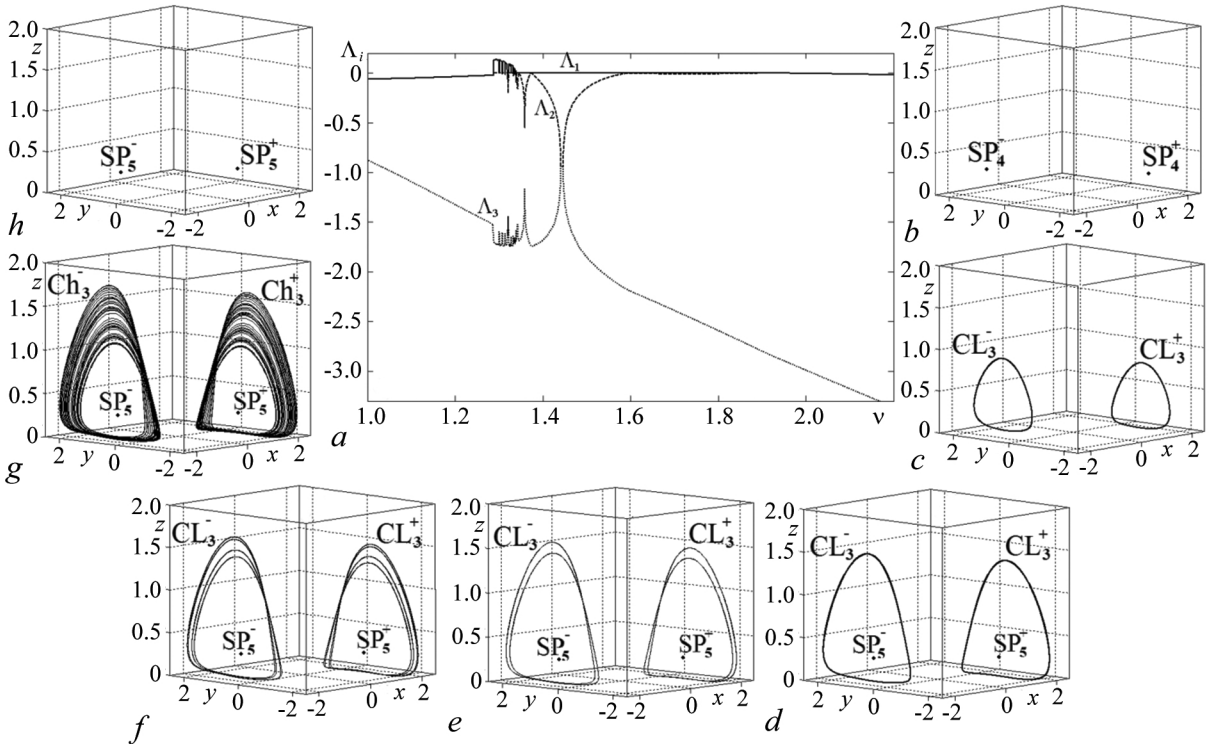

Fig. 7. *a* — Graphs of Lyapunov exponents of the model (11) on the parameter ν at $\gamma = 0.5$. *b*–*h* — Attractors of the model (11) at $\gamma = 0.5$: $\nu = 2.2$ (*b*); 1.6 (*c*); 1.4 (*d*); 1.36 (*e*); 1.34 (*f*); 1.3 (*g*); 1.2 (*h*)

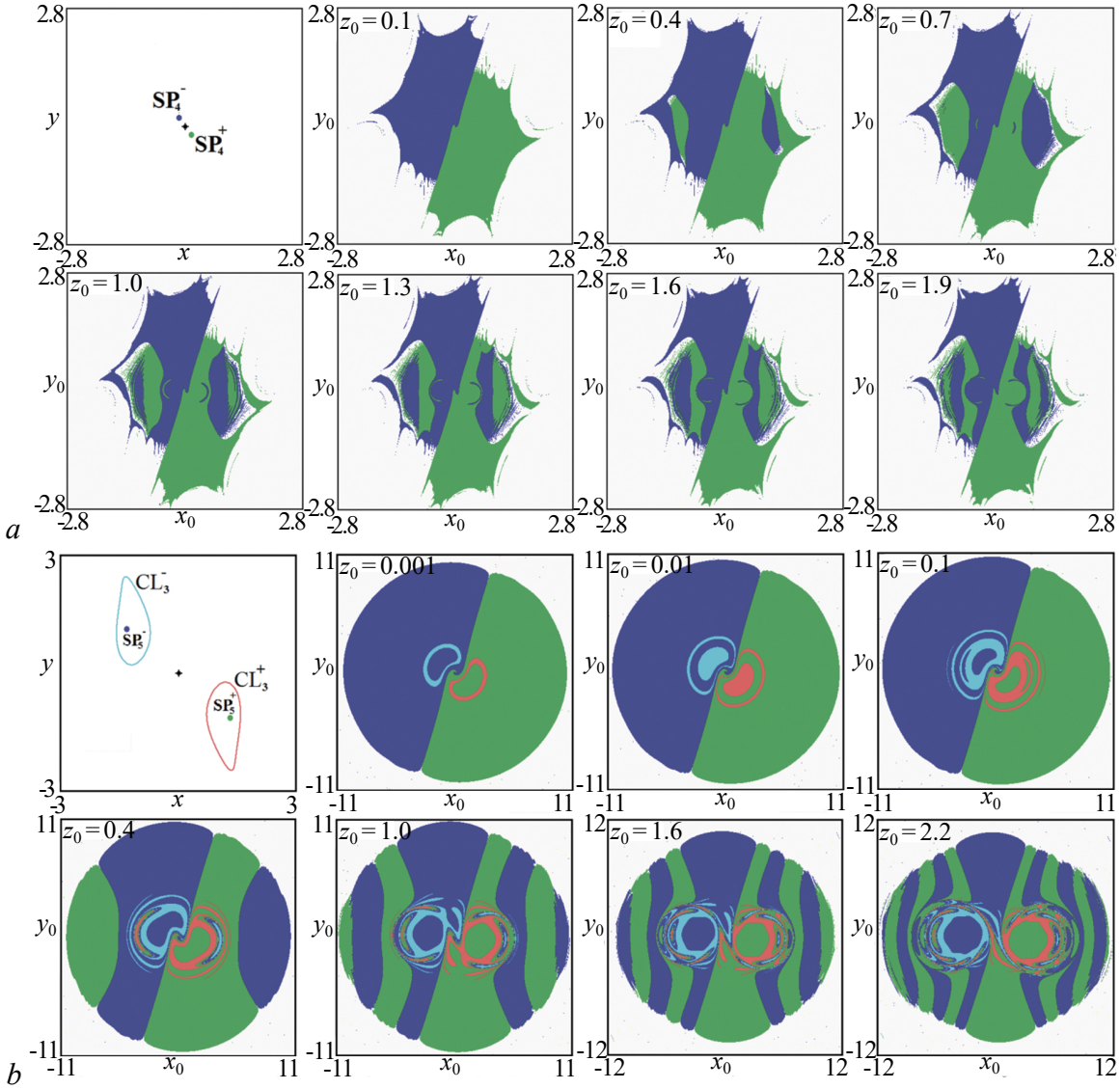

Fig. 8. Projection of the attractors on a (x, y) plane and sections of their basins of attraction by the $z_0 = \text{const}$ plane plotted for the model (11), $\gamma = 0.5$: $\nu = 2.2$ (a), $\nu = 1.4$ (b). The basins of SP_4^- and SP_5^- are colored blue, the basins of SP_4^+ and SP_5^+ are colored green, the basin of CL_3^- is colored light blue and the basin of CL_3^+ is colored red (color online)

observed at $\gamma = 0.78$ (see fig. 6, a), a circle of a rather large radius, which is divided into two parts by manifolds of an unstable equilibrium position located at the origin. With the growth of z_0 new regions appear both outside and inside the circle, representing the basins of attraction of the symmetric attractor (equilibrium positions).

Now consider the pools of attraction of limit cycles CL_3^- and CL_3^+. Their arrangement and transformation are identical to those observed for the limit cycles of CL_2^- and CL_2^+ for $\gamma = 0.78$ (see fig. 6, b). In contrast to the above case, the pools of attraction of limit cycles CL_3^- and CL_3^+ they exist at arbitrarily small values of z_0, and their transformation is faster. Also the pools of attraction of limit cycles CL_3^- and CL_3^+ they are always located inside the central pools of attraction of the equilibrium positions SP_5^- and SP_5^+.

Note that, as in the previous case ($\gamma = 0.78$), the pools of attraction of limit cycles CL_3^- and CL_3^+, observed at those values of the parameter ν when in the system (11) there is no

multistability, for example at $\nu = 1.6$ (see Fig. 7, *c*), identical to the pools of attraction shown in Fig. 8, *a*. The pools of attraction for all other modes, in cases where there is multistability (see Fig. 7, *d*–*g*), are identical to the pools of attraction shown in Fig. 8, *b*. A pools of attraction for stable equilibrium positions SP_5^- and SP_5^+ (see Fig. 7, *h*) are qualitatively identical to those observed for stable equilibrium positions SP_2^- and SP_2^+, systems (11) for $\gamma = 0.78$ (see Fig. 6, *a*) with the only difference that in this case the transformation of pools occurs faster, and their size grows slower.

Thus, the system (11) at $\gamma = 0.5$ demonstrates dynamics identical to that observed in it for $\gamma = 0.78$. The difference is that the pools of attraction of stable equilibrium positions have a different device. At the same time, the dynamics of the system (11) at $\gamma = 0.5$ is similar to the dynamics of the Rabinovich – Fabricant model (1), except for the device of the attractor attraction pools [20].

4.4. The case of small values of parameter γ. And finally, consider the case of small values of the parameter γ: $\gamma = 0.2$ and $\gamma = 0.1$. Just as in the Rabinovich model–Fabricant (1), in the system (11), two structures corresponding to the existence of different types of limit cycles will be observed on the map of dynamic modes in this area (compare Fig. 2, *a* and fig. 2, *c*). The right structure corresponds to the fact that the stable equilibrium positions of SP existing at large values of the parameter ν_6^- and SP_6^+ (fig. 9, *a*) when it is reduced as a result Andronov –Hopf bifurcations become unstable, and limit cycles CL are born in the system$_4^-$ and CL_4^+ (fig. 9, *b*). With a further decrease in the parameter ν, a transition to chaos occurs through a sequence of period doubling bifurcations (Fig. 9, *c*–*e*). At the same time, the attraction pools of the observed attractors are completely identical to those observed in the system (11) for the equilibrium positions of SP_4^- and SP_4^+ (fig. 8, *a*) for $\gamma = 0.5$.

The second (left) structure corresponds to the fact that at first in the phase space of the system (11) there is not a pair of symmetrically arranged limit cycles, but one symmetric limit cycle CL_7, which, when replacing the variables x by $-x$ and y by $-y$ passes into itself (fig. 9, *f*). When the parameter ν decreases, a pair of symmetrically arranged limit cycles CL occurs inside this cycle$_8^-$ and CL_8^+, coexisting with the CL_7 cycle (fig. 9, *g*). At the same time, the cycle CL_7 retains its symmetry. With a further decrease in the parameter ν, the limit cycle CL_7 loses symmetry and demonstrates a transition to chaos through a sequence of period doubling bifurcations (Fig. 9, *h*). At the same time, the limit cycles of CL coexisting with it$_8^-$ and CL_8^+ they decrease in size and disappear, instead of them a pair of symmetrically arranged stable equilibrium positions is born.$_7^-$ and SP_7^+ (fig. 9, *i*). And finally, the chaotic attractor disappears,

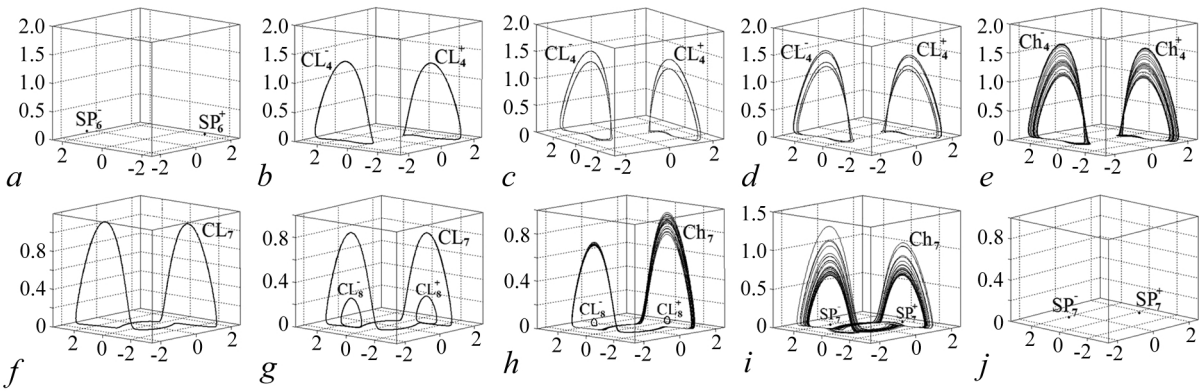

Fig. 9. Attractors of the model (11) at $\gamma = 0.2$: 2.3 *a*; 1.6 (*b*); 1.55 (*c*); 1.543 (*d*); 1.53 (*e*) and at $\gamma = 0.1$: $\nu = 1.6$ (*f*); 1.4 (*g*); 1.31 (*h*); 1.29 (*i*); 1.2 (*j*)

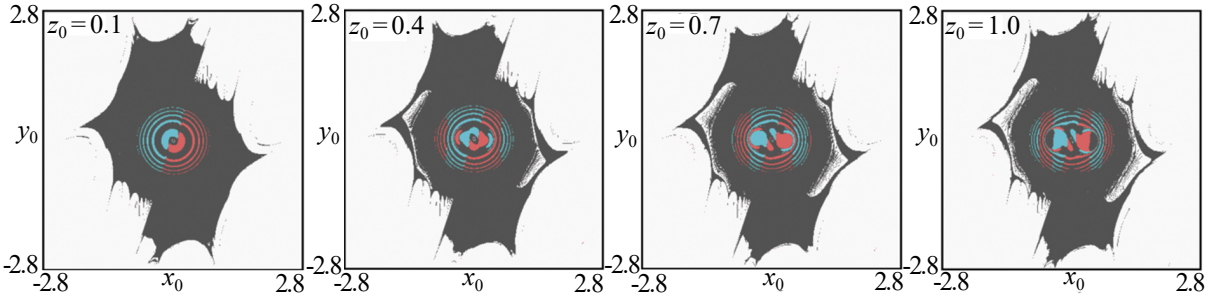

Fig. 10. Sections of the basins of the attractors by the $z_0 = \text{const}$ plane plotted for the model (11), $\gamma = 0.1$ and $\nu = 1.4$. The basin of CL_7 is colored grey, the basin of CL_8^- is colored light blue and the basin of CL_8^+ is colored red (color online)

and only stable equilibrium positions of SP are observed in the phase space of the system $(11)_7^-$ and SP_7^+ (see fig. 9, *j*).

Thus, the dynamics of the system (11) with small parameter values γ is identical to the dynamics of the Rabinovich – Fabricant model(1) for the same parameter values. But the attraction pools of the attractors will differ significantly. In the case when there is no multistability in the system (11), (see Fig. 9, *a*–*f*, *j*) the pools of attraction are identical (both qualitatively and quantitatively) to the pools of attraction of stable equilibrium positions SP_4^- and SP_4^+ for $\gamma = 0.5$ (see fig. 8, *a*). And when multistability is present in the system (11) (see Fig. 9, *g*–*i*) The pools of attraction will have the form shown in Fig. 10. Here, the pool of attraction of the limit cycle CL_7 is colored gray and identical to what was observed in the absence of multistability. Pools of attraction of limit cycles CL_8^- and CL_8^+ they are circles and «islands» located inside the pool of attraction of the limit cycle CL_7.

4.5. Bifurcation analysis of a generalized system. In conclusion, a numerical search for bifurcation lines for equilibrium positions and limit cycles of period one was carried out for the system (11) using the MatCont program. The corresponding bifurcation diagram is shown in Fig. 11. It agrees well with the map of dynamic modes presented in Fig. 2, *c*, confirms its structure and describes in more detail the variants of multistability observed in the system. It can also be used to determine the total number of stable equilibrium positions and limit cycles of period one arising in the system under consideration.

Note that in many ways the bifurcation pattern of the system (11) on the plane (ν, γ) is similar to the one that took place for the Rabinovich – Fabricant model (1) [20]. So, first of all, when moving along the plane from right to left, first on the SN line, as a result of saddle-node bifurcation, a stable and unstable equilibrium position is born.We remind you that all equilibrium positions and cycles in the system (11) are born in symmetric pairs.. Further, the stable equilibrium position becomes unstable on the H_1 line, as a result of the Andronov –Hopf bifurcation. At the same time, a stable limit cycle is born in the system, the period of which doubles on the bifurcation line of the doubling of the PD period (Fig. 11). As follows from the view of the dynamic mode map (see Fig. 2, *c*), then there will be a cascade of period doubling bifurcations, as a result of which a chaotic attractor appears in the system (11). This coincides with what was observed in the Rabinovich – Fabricant model (1) in the same region of the parameter space.

Secondly, when moving along the plane of the parameters (ν, γ) from left to right in the region $\gamma < 0.94$ on the line H_2 as a result of the inverse bifurcation of Andronov–Hopf, a stable position

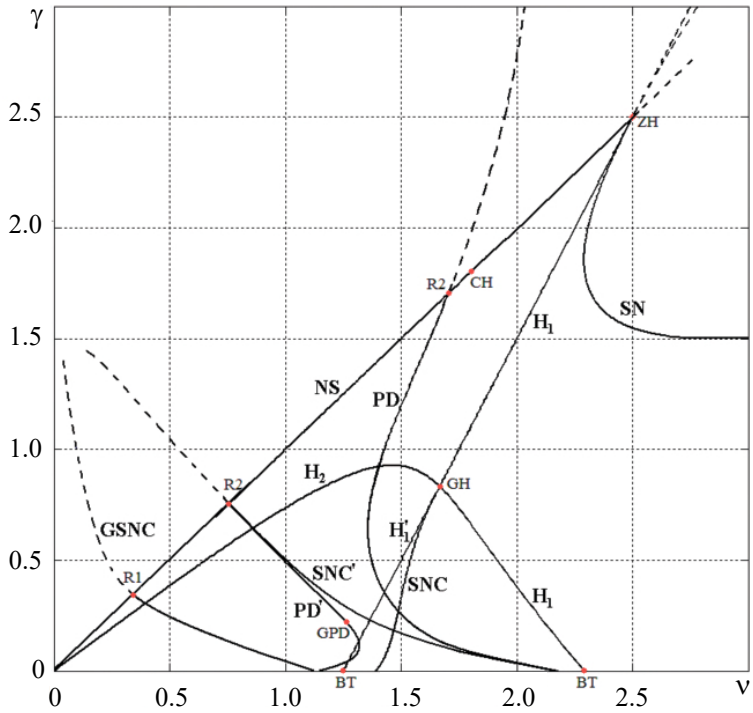

Fig. 11. Bifurcations lines and points of the general model (11) on the (ν, γ) parameter plane, $p = 0.9$ and $q = 0.1$. SN is saddle-node bifurcation of the stable point, SNC is saddle-node bifurcation of the limit cycle, H_1 is direct Hopf bifurcation, H_2 is inverse Hopf bifurcation, PD is period doubling bifurcation of the limit cycle, GSNC is hard saddle-node bifurcation of the limit cycle, NS is inverse Neimark–Saker bifurcation, GH is generalized Hopf bifurcation point, GPD is generalized period doubling bifurcation point, ZH is Zero–Hopf bifurcation point, R1 is resonance 1:1, R2 is resonance 1:2, BT is Bogdanov–Takens bifurcation point. The bifurcation lines corresponded unstable regimes are indicated by dotted lines

is born equilibria and unstable limit cycle. Then this stable equilibrium position will become unstable on the H line$_1'$ as a result of Andronov's direct bifurcation–Hopf, and a stable limit cycle will arise in the system, which will disappear as a result of saddle-node bifurcation of limit cycles on the SNC line, merging with an unstable limit cycle, born as a result of Andronov's inverse bifurcation–Hopf on the line H_2 (Fig. 11). At the same time, since the lines H_1' and SNC, in a certain region of the parameter space are between the lines PD and H_1, then several types of multistability are possible in the system (11), when a stable limit cycle with different periods or does chaos coexist with a stable equilibrium position or with a stable limit cycle of period one.

Thirdly, when moving along the plane of parameters (ν, γ) from right to left in the region $\gamma < 0.3$ and $\nu < 2.0$ on the line SNC$'$ as a result of saddle-node bifurcation of limit cycles, stable and unstable limit cycles are born, passing into themselves when replacing the variables x with $-x$ and y with $-y$ (see Fig. 9, f). Further on the PD$'$ line, the period of the steady cycle will double (see Fig. 11) and in the future, as follows from the view of the dynamic mode map (Fig. 2, c), there will be a cascade of period doubling bifurcations, as a result of which chaos occurs in the system (11). At the same time, since the lines H_1' and SNC intersect the domain of existence of the specified cycle, then multistability is possible in the system under consideration when a stable limit cycle co-exists in the phase space, passing into itself when variables are replaced, and a symmetric pair of stable limit cycles of period one (see Fig. 9, g).

Thus, the following attractors are observed in the system (11): two pairs of stable equilibrium positions and two pairs of stable limit cycles resulting from different bifurcations, and a symmetric

limit cycle. A the rather complicated arrangement of bifurcation lines presented in Fig. 11 leads to a large number of combinations of their mutual coexistence.

However, in the bifurcation picture of the system (11) there are a number of differences from the system (11). Thus, two new bifurcation lines are observed in the system (11), which were not present in the Rabinovich – Fabricant model (1) [20]. These are the GSNC line, on which there is a rigid tangent bifurcation of limit cycles, and the NS line, on which there is an inverse Neumark bifurcation–A Saker that bounds on the plane of parameters (ν, γ) the area of existence of periodic regimes and chaos on the left. Also, several bifurcation points of codimension two appeared in the system (11). This is the GPD point, which is a generalized period doubling bifurcation point, ZH— the intersection point of the tangent bifurcation line of the fixed point and the Andronov bifurcation line–Hopf (Zero bifurcation point–Hopf), R1 and R2 corresponding to the resonances of $1:1$ and $1:2$, respectively.

Another difference between the bifurcation pattern of the system (11) and the one that took place in the Rabinovich model– Fabricant (1) is that in the Rabinovich model–Fabricant (1) had two GH points (generalized Andronov bifurcation point–Hopf). In the first, the lines of the direct Andronov bifurcation–Hopf converged, the reverse Andronov bifurcation–Hopf and saddle-node bifurcation of limit cycles converged, and in the second — two lines of the direct Andronov bifurcation–Hopf and two Andronov inverse bifurcation lines–Hopf [20]. In the system (11), these two points have merged, and only one point GH is observed, to which five lines converge: two lines H_1, line H_1' (all correspond to the direct Andronov bifurcation–Hopf), the H_2 line (inverse Andronov bifurcation–Hopf) and the SNC line (saddle-node bifurcation of limit cycles) (see Fig. 11).

Conclusion

In the work, within the framework of the Lagrange formalism, a three-mode interaction in the presence of a cubic nonlinearity of a general form is considered. An initial system consisting of three oscillators was recorded, for which analytically, using the method of slowly varying amplitudes, a three-dimensional system was obtained, which is a generalization of the Rabinovich – Fabricant model for the case under consideration.

The dynamics of the resulting system is investigated numerically using methods of dynamic chaos theory. For it, maps of dynamic modes are constructed both on the plane of parameters representing dissipation coefficients and on the plane of parameters characterizing the nonlinear interaction between oscillators in the system; the dependences of Lyapunov exponents on the parameter, attractors and their pools of attraction. The main bifurcations of equilibrium positions and limit cycles of period one are found. A comparison was made with the Rabinovich – Fabricant model: the values of the parameters of nonlinear interaction were indicated, at which the equations of the resulting system completely coincide with the equations for the Rabinovich – Fabricant modelFabricant model. In the case when the equations do not coincide, the regions in the parameter space are indicated for which the dynamics of the resulting model is completely or partially identical to the dynamics of the Rabinovich – Fabricant model.

The study showed that the arrangement of the plane of parameters characterizing the nonlinear interaction between the oscillators does not depend on the parameters representing the dissipation coefficients, but is determined by the ratio between the parameters of nonlinearity themselves. But the arrangement of the plane of parameters representing the dissipation coefficients depends significantly on the parameters of the nonlinear interaction. So, if the parameter $q = 0$, then the dynamics of the system under consideration is identical to the dynamics of the Rabinovich

– Fabricant model, although their equations do not coincide. In this case, the model under consideration turns into the Rabinovich – Fabricant model when $p = 1$ и $q = 0$.

In the region of $p + 3q > 0$, $3p + q > 0$ and $q > 0$, the dynamics of the system under consideration is qualitatively as similar as possible to the dynamics of the Rabinovich –Fabricant model, although it demonstrates a number of differences: an increase in the multistability region, the appearance of new bifurcation lines and there are two codimension points, etc., etc. In all other areas, the dynamics of the system under consideration differs significantly from the dynamics of the Rabinovich – Fabricant model up to the disappearance of some structures or the appearance of new ones.

References

1. Kuznetsov SP. Dynamical Chaos. Moscow: Fizmatlit; 2006. 356 p. (in Russian).
2. Ott E. Chaos in Dynamical Systems. Cambridge: Cambridge University Press; 1993. 385 p.
3. Guckenheimer J, Holmes PJ. Nonlinear Oscillations, Dynamical Systems, and Bifurcations of Vector Fields. New York: Springer-Verlag; 1983. 462 p. DOI: 10.1007/978-1-4612-1140-2.
4. Anishchenko VS, Vadivasova TE, Astahov VV. Nonlinear Dynamics of Chaotic and Stochastic Systems. Saratov: Saratov University Publishing; 1999. 367 p. (in Russian).
5. Schuster HG, Just W. Deterministic Chaos: An Introduction. Weinheim: Wiley; 2005. 287 p. DOI: 10.1002/3527604804.
6. Kuznetsov SP. Dynamical Chaos and Hyperbolic Attractors: From Mathematics to Physics. Moscow-Izhevsk: Institute for Computer Research; 2013. 488 p. (In Russian).
7. Neimark JI, Landa PS. Stochastic and Chaotic Oscillations. Dordrecht: Springer; 1992. 500 p. DOI: 10.1007/978-94-011-2596-3.
8. Lorenz EN. The Essence of Chaos. Seattle, WA, USA: University of Washington Press; 1995. 240 p.
9. Alligood KT, Sauer T, Yorke J. Chaos: An Introduction to Dynamical Systems. New York: Springer-Verlag; 1996. 603 p. DOI: 10.1007/b97589.
10. Hilborn RC. Chaos and Nonlinear Dynamics: An Introduction for Scientists and Engineers. Oxford: Oxford University Press; 2001. 672 p.
11. Rabinovich MI, Fabrikant AL. Stochastic self-modulation of waves in nonequilibrium media. Sov. Phys. JETP. 1979;77(2):617–629 (in Russian).
12. Danca MF, Feckan M, Kuznetsov N, Chen G. Looking more closely to the Rabinovich–Fabrikant system. International Journal of Bifurcation and Chaos. 2016;26(2):1650038. DOI: 10.1142/S0218127416500383.
13. Liu Y, Yang Q, Pang G. A hyperchaotic system from the Rabinovich system. Journal of Computational and Applied Mathematics. 2010;234(1):101–113. DOI: 10.1016/j.cam.2009.12.008.
14. Agrawal SK, Srivastava M, Das S. Synchronization between fractional-order Rabinovich–Fabrikant and Lotka–Volterra systems. Nonlinear Dynamics. 2012;69(4):2277–2288. DOI: 10.1007/s11071-012-0426-y.
15. Srivastava M, Agrawal SK, Vishal K, Das S. Chaos control of fractional order Rabinovich–Fabrikant system and synchronization between chaotic and chaos controlled fractional order Rabinovich–Fabrikant system. Applied Mathematical Modelling. 2014;38(13):3361–3372. DOI: 10.1016/j.apm.2013.11.054.
16. Danca MF. Hidden transient chaotic attractors of Rabinovich–Fabrikant system. Nonlinear Dynamics. 2016;86(2):1263–1270. DOI: 10.1007/s11071-016-2962-3.
17. Danca MF, Kuznetsov N, Chen G. Unusual dynamics and hidden attractors of the Rabinovich –Fabrikant system. Nonlinear Dynamics. 2017;88(1):791–805. DOI: 10.1007/s11071-016-3276-

1.
18. Danca MF, Chen G. Bifurcation and chaos in a complex model of dissipative medium. International Journal of Bifurcation and Chaos. 2004;14(10):3409–3447. DOI: 10.1142/S0218127404011430
19. Luo X, Small M, Danca MF, Chen G. On a dynamical system with multiple chaotic attractors. International Journal of Bifurcation and Chaos. 2007;17(9):3235–3251. DOI: 10.1142/S0218127407018993.
20. Kuznetsov AP, Kuznetsov SP, Turukina LV. Complex Dynamics and Chaos in the Rabinovich–Fabrikant Model. Izvestiya of Saratov University. Physics. 2019;19(1):4–18 (in Russian). DOI: 10.18500/1817-3020-2019-19-1-4-18.
21. Hocking LM, Stewartson K. On the nonlinear response of a marginally unstable plane parallel flow to a two-dimensional disturbance. Proc. R. Soc. Lond. A. 1972;326(1566):289–313. DOI: 10.1098/rspa.1972.0010.
22. Andronov AA, Fabrikant AL. Landau damping, wind waves and whistle. In: Nonlinear Waves. Moscow: Nauka; 1979. P. 68–104 (in Russian).
23. Kuramoto Y, Yamada T. Turbulent state in chemical reactions. Progress of Theoretical Physics. 1976;56(2):679–681. DOI: 10.1143/PTP.56.679.